On Some Trends Associated with Stage II Fatigue Crack Growth Behavior of Metals

Tawfik M. Ahmed[1], Desmond Tromans[2]
[1] *Ionik Consulting/JP Kenny Inc., Houston, TX, USA;* [2] *Department of Materials Engineering, University of British Columbia, BC, Canada*

Abstract

Experimental data from the literature for a wide group of metallic materials including steel, titanium, copper, and aluminum alloys obtained under a wide range of fatigue testing conditions were examined for common trends associated with Stage II fatigue crack growth rates. Among these trends, the correlation between the striation data and Young's modulus (*E*). Also, the linear relation between Paris parameters (*m* vs. log *C*) and its correlation with Young's modulus. These trends are discussed in reference to fatigue crack growth rates under closure-free conditions. The results emphasize the importance of *E* on fatigue crack growth behavior of metallic materials and provide a basis to predict fatigue life of engineering components under various conditions. Comparisons are made with crack growth equations that are commonly employed in damage tolerance analyses.

1 Introduction

Numerous experimental data for a wide range of different metals and alloys have confirmed that the Paris region crack growth rates are directly related to ΔK by an empirical relation known as the Paris relationship, or sometimes, as the Paris-Erdogan relationship [1]:

$$\frac{da}{dN} = C\Delta K^m \tag{1}$$

where *C* and *m* are scaling constants, *m* is the slope of the Paris region and *C* is the intercept at ΔK equal to 1.

The parameters *m* and *C* in the Paris relationship show some sensitivity to environmental and experimental conditions, and the metallurgical and mechanical properties of the material tested. Although, many efforts have been made to model fatigue crack growth rates (FCGR) and predict the values of *m* and *C*, modeling has proven to be challenging due to the complexity and difficulty in quantifying crack closure. Crack closure effects have been shown to play a significant role in affecting the FCGR and, consequently, the values of *m* and *C*. Predictions of Paris parameters would be less challenging if made for closure-free conditions, i.e., $\Delta K \approx \Delta K_{eff}$. Many investigators demonstrated a good correlation between

FCGR and the ratio $\Delta K/E$, particularly under closure-free behavior [2-4]. Hertzberg [5] showed this correlation is most relevant under closure free conditions and he established a simple relationship to estimate FCGR under closure-free conditions in the following form:

$$\frac{da}{dN} = \frac{1}{\sqrt{b}} \cdot \left(\frac{\Delta K}{E} \right)^3 = \frac{1}{\sqrt{b}} \cdot \left(\frac{\Delta K_{eff}}{E} \right)^3 \tag{2}$$

where b is Burgers vector which is based on the atom diameter as calculated from the crystal structure.

A closer examination of Hertzberg's relation suggests E is the key factor in controlling FCGR as b does not change significantly for different metals, i.e., b ranges approximately from 2.5×10^{-10} to 3.0×10^{-10} m [5]. Thus, based on an average b value of 2.75×10^{-10} m, Hertzberg's relation can be rewritten with a coefficient of $\sim 6\times10^7$ as:

$$\frac{da}{dN} \approx 6\times10^7 \left(\frac{\Delta K_{eff}}{E} \right)^3 \tag{3}$$

Hertzberg's relation implies that changing the microstructure of a material, which generally affects mechanical properties without significant effect on E, may not impact FCGR significantly and hence material's fatigue resistance under high operating R (R is the load ratio defined as P_{min}/P_{max} and it is referred to here as R-ratio). At high R-ratios fatigue cracks are known to grow under closure free.

Furthermore, it has been shown that the parameters m and C are inter-related for a wide variety of materials [6,7-17]. A *log*-linear relationship has been observed for a given material under different testing conditions such that:

$$\log(C) = \alpha m + \beta \tag{4}$$

where α and β are the coefficients of the regression line (α is the slope and β is the intercept at $m = 0$), as shown schematically in Fig. 1. Hickerson and Hertzberg [7] pointed out that the correlation in Eq. (4) is a result of the fact that different slopes of the Paris region obtained under different test conditions tend to converge to a single point, termed the pivot point, shown in Fig. 1. One implication of this convergence is that curves of higher growth rates are always associated with lower values of m.

Tanaka *et al.* [6] indicated that the pivot points for steel, titanium, and aluminum alloys occurred consistently within ΔK range where striation became visible on fatigue fracture surfaces. Tanaka *et al.* [6] believed that the typical fatigue fracture mechanism (striation formation) operates most strongly in the vicinity of the pivot point. Iost and Lesage [11] reviewed pivot points for an extensive range of steel, titanium, copper, and aluminum alloys from more than 30 publications conducted under different testing conditions. They showed graphically that a correlation existed between $(da/dN)_{pp}$ vs. ΔK_{pp} on logarithmic axes of $(da/dN)_{pp}/b$ vs. $\Delta K_{pp}/E\sqrt{b}$.

The extensive work of Tanaka *et al.* [6], and Bates and Clark [18] is of particular interest. These workers examined independently the relationship between striation spacing (da/dN) and ΔK level at which they become visible on the fatigue fracture surfaces for several structural alloys including steel, titanium and aluminum alloys tested at different R-ratios including $R = 0$. They showed a good correlation between FCGR and the ratio $\Delta K/E$. It was interesting to see all their striations data fell within a scatter band when ΔK was normalized with respect to E.

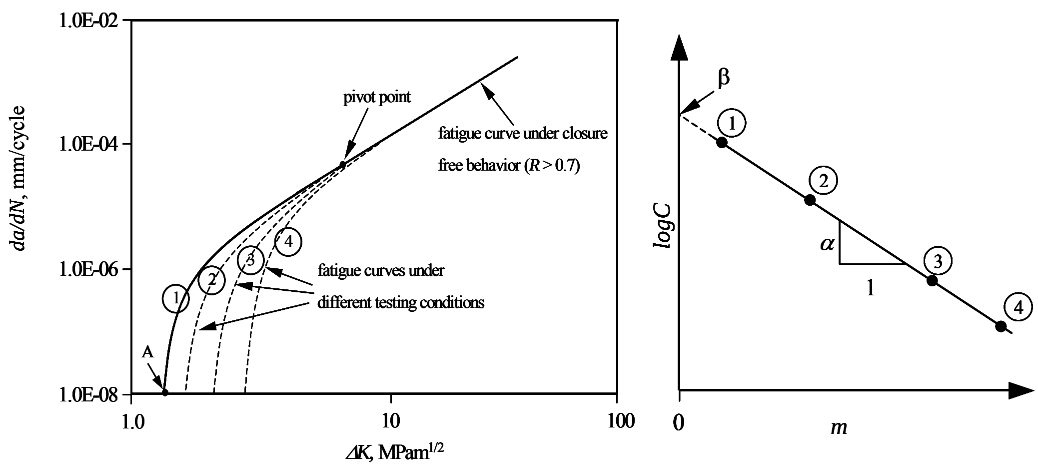

Fig. 1: Schematic representation of the pivot point and the relation between m and $log(C)$ for a given material when tested for instance under different R-ratios.

The aim of the present work is to examine closely the correlation of FCGR to the ratio $\Delta K/E$ that was observed for closure-free behavior, pivot points and striation data for different metals. Efforts were made to explore these correlations and determine its importance and implications.

2 Linear Relation Between ΔK_{pp} and $(da/dN)_{pp}$

Iost and Lesage [11] reviewed pivot points for an extensive range of steel, titanium, copper, and aluminum alloys. They showed graphically that a correlation existed between $(da/dN)_{pp}$ vs. ΔK_{pp} on logarithmic axes of $(da/dN)_{pp}/b$ vs. $\Delta K_{pp}/E\sqrt{b}$. However, for the purpose of this study their data were shown on logarithmic axes of $(da/dN)_{pp}$ vs. $\Delta K_{pp}/E$. Fig. 2 shows all the data collected by Iost and Lesage [11]. Several more data points were included from recent publications [8,12-14]. The selected E values for all the alloys are listed in Table 1 which are based on E of the principal alloying elements (e.g., Al in Al-based alloys, Cu in Cu-based alloys, Ti in Ti-based alloys, and Fe in Fe-based alloys). It is recognized that there will be slight differences in E between different alloys in the same metal-based system, but such differences would have insignificant impact on Sage II *da/dN*.

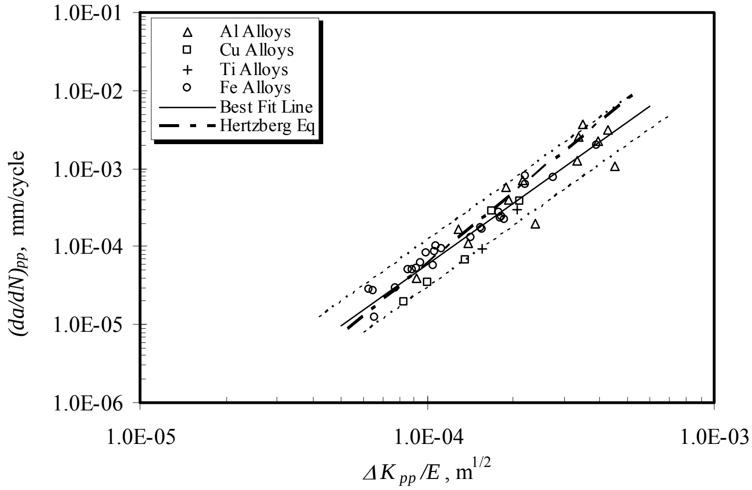

Fig. 2: Pivot point data for aluminum, copper, titanium and steel alloys are normalized with respect to *E* and plotted on logarithmic scale.

Table 1: Magnitude of Burgers vector (*b*) and elastic modulus (*E*) used to calculate Hertzberg's relation.

Alloy	b [10^{-10} m]	E [GPa]	$C = \frac{1}{\sqrt{b}E^3}$
Aluminum	2.86	70	1.72×10^{-7}
Copper	2.56	120	3.62×10^{-8}
Titanium	2.95	117	3.73×10^{-8}
Steel	2.48	200	7.94×10^{-9}

Every single datum point in Fig. 2 represents a whole fatigue study by itself that included, in some cases, about twenty fatigue tests conducted on a given alloy under different testing conditions. It is evident from Fig. 2 that when ΔK_{pp} is normalized with respect to *E* for the base metal, data for the different alloys tend to fall on the same straight line within a relatively narrow scatter band. It is quite impressive to see all these alloys with diverse metallurgical and mechanical properties tested under different conditions exhibit such consistency. Two aluminum points deviated notably from the others, which could be related to the lack of sufficient data or difficulties in estimating *m* and *C*, i.e., in some instances, the experimental data of Stage II show significant curvature which can affect the slope of *m* and makes its value greatly dependent on the range of ΔK considered.

3 Correlation with FCGR under Closure-Free Conditions

Linear regression was carried out on the data of Fig. 2 and a best fitting line obtained (solid line in Fig. 2):

$$\left(\frac{da}{dN}\right)_{PP} = 1.6\times10^{6}\left(\frac{\Delta K_{PP}}{E}\right)^{2.6} \tag{5}$$

when $(da/dN)_{PP}$ is expressed in mm/cycle and ΔK_{PP} in MPa√m. Note the resemblance of Eqs. (3) and (5). Therefore, an argument can be that the data in Fig. 2 represent the FCGR behavior under closure-free conditions. Hertzberg's prediction line for closure-free behavior is included for comparison in Fig. 2, where this line was based on Eq. (3). It is evident that a great similarity exists between the normalized ΔK_{pp} data in Fig. 2 and Hertzberg's relation. In fact, Hertzberg's prediction line was almost identical to the best fit line of the pivot points obtained via Eq. (5).

One significant implication to be drawn from Fig. 2 is that the pivot points for any group of alloys in a common alloy system (steel, Cu-based, Ti-based, or aluminum-based alloys) always fall on a line that represents FCGR under closure-free conditions (the upper bound for FCGR). This upper bound is identical for this group of alloys regardless of what the composition, metallurgical and experimental conditions are, as was implicated earlier by Hertzberg's relation. As a result, Fig. 2 confirms the notion that modifications in the alloy's composition, microstructure or mechanical properties affect the fatigue behavior at the threshold and near-threshold regions by contributing to different crack closure processes [16,17]. As ΔK is increased beyond the threshold region, crack closure gradually diminishes and FCG become closure free. This leads to the very important conclusion that variations in the ΔK_{PP} values for any alloy system (steel, Cu-based, or Al-based alloys) are due to the differences in the extent of crack closure contribution from one alloy to another under different experimental conditions. This will be more evident in Section 5. This finding is not well recognized in the fatigue literature and could have important implication on the development of alloys with better fatigue crack growth resistance.

4 Correlation with Striation Spacing

Fractographic studies reveal that striation spacing commonly reflects the incremental advance of the crack front resulting from one loading cycle (striation spacing is equivalent approximately to *da/dN*). In Fig. 3, the striation data reported by Tanaka *et al.* are compared with the line corresponding to Hertzberg's equation and with the scatter band obtained from Fig. 2. Most of the striation data fall within the scatter band with some points deviating slightly out of the band. In view of the good agreement in Fig. 3, it is reasonable to assume that the correlation of striation spacing with respect to E cited by Tanaka *et al.* [6], and Bates and Clark [18] originated from the fact that their striation data correspond to FCGR under closure-free conditions i.e., striations become visible under closure-free behavior.

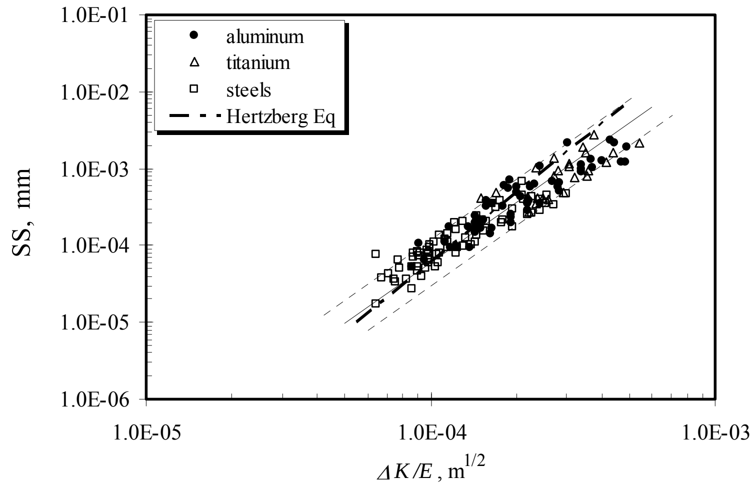

Fig. 3: Striation spacing data [6] for different structural alloys are compared with Hertzberg's line and the scatter band of the pivot points of Fig. 2.

Knowing the fact that some of the striation data were obtained at zero *R*-ratio, Fig. 3 confirms the notion that closure processes become insignificant at high ΔK values, i.e., striation spacing is insensitive to *R*-ratio at high ΔK and depends on the value of ΔK and the class of alloy (steel, Cu-based, Ti-based, or Al-based alloys). Additionally, the trends in Fig. 3 have an important implication. They imply that striation spacing is independent of the metallurgical structure of the material, as was the case for closure-free behavior, and as was reported in the literature [6].

5 Some Considerations on the *m* vs. *log*(*C*) Relation

An assessment of the published fatigue data [19-21] related to the current work has shown that the real FCGR curves for a given material under different testing conditions in many cases converge to a common single point. It is interesting to note that several studies on a wide range of steels including ferritic-pearlitic, ferritic-bainitic, fully bainitic, and fully martensitic microstructures in moist and dry environments at different *R*-ratios have shown similar behavior to those shown in Fig. 1. This behavior is explained through the effects of closure processes, particularly the oxide-induced closure and roughness-induced closure [21]. For instance, Fig. 4 shows fatigue crack growth curves for pressure vessel martensitic steel (2 ¼ Cr- 1Mo steel, σ_{ys} = 769 MPa) tested in moist air and dry hydrogen gas at R = 0.05 and 0.75 (50 Hz) [22]. The lines of Eqs. (2) and (5) are shown in Fig. 4 where they compare reasonably well with the fatigue curve at 0.75 *R*-ratio (closure-free curve). At R = 0.05, fatigue curves in air and dry hydrogen started with higher threshold values and gradually approached the air curve of R = 0.75 as ΔK was increased. The values of *m* and *C* were calculated for the four curves and these are shown on semi-logarithmic axes in Fig. 4, along with the equation of the best fit line.

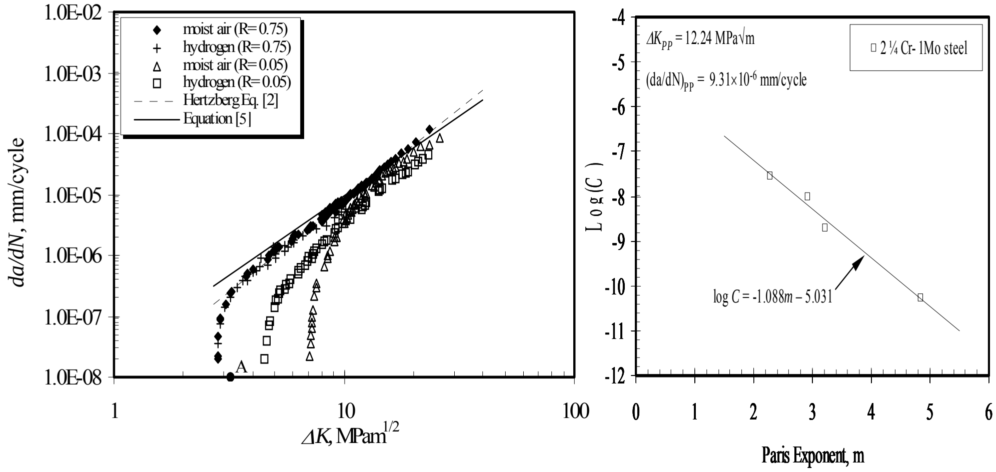

Fig. 4: Fatigue crack growth curves of pressure vessel martensitic steel (2 ¼ Cr-1Mo steel) tested in moist air and dry hydrogen gas at $R = 0.05$ and 0.75 [22].

Changing the steel composition will lead to a convergence of fatigue curves at higher ΔK and *(da/dN)* but is still along the line of Eq. (5). Fig. 5 shows this shift in martensitic 300 M-T650 steel (σ_{ys} = 1070 MPa) tested in moist air and dry hydrogen at $R = 0.05$ and 0.75 (50 Hz) [23]. The shift to higher ΔK value is an indication of increased contribution of the closure process, i.e., oxide-induced closure in this case [23], as evidenced by the lower FCGR at $R = 0.05$ when

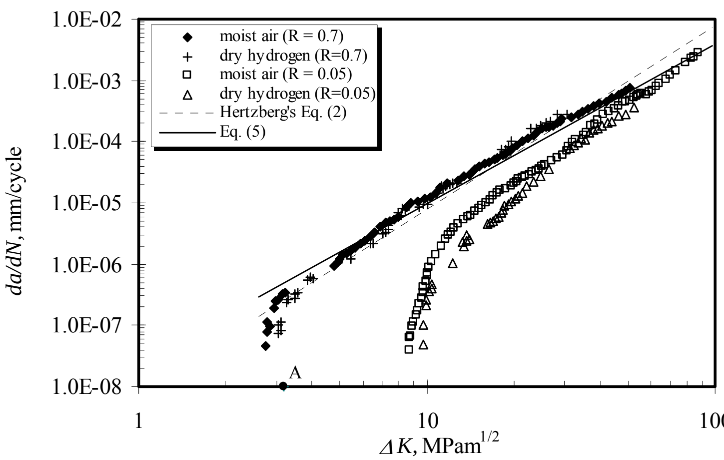

Fig. 5: Fatigue crack growth curves of martensitic 300M-T650 steel tested in moist air and dry hydrogen gas at $R = 0.05$ and 0.75 (50 Hz) [23].

compared to those of Fig. 4. Note the air curves at $R = 0.75$ in Fig. 4 and Fig. 5 are almost identical and in agreement with Eqs. (2) and (5). The convergence of fatigue curves and the remarkable correlations with Eqs. (2) and (5) were also found for 2219-T851 aluminum alloy (σ_{ys} = 350 MPa) and Ti-6Al-4V alloy (σ_{ys} = 774 to 848 MPa), as can be seen in Fig. 6 [24] and Fig. 7 [25], respectively.

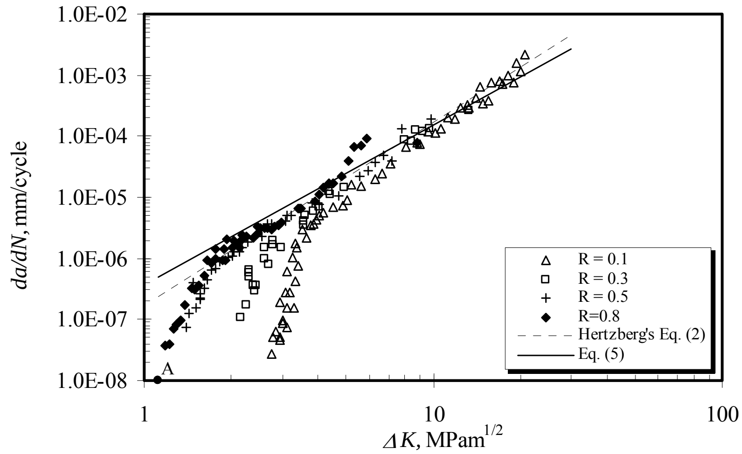

Fig. 6: Fatigue curves for 2219-T851 aluminum alloy in ambient air at different R-ratios [24].

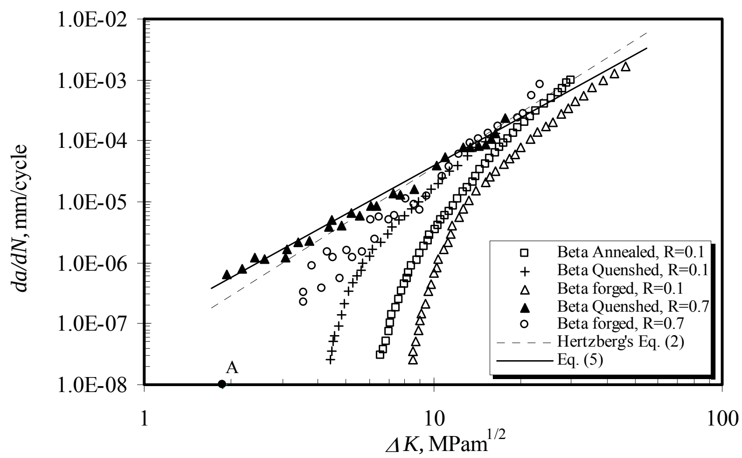

Fig. 7: The effects of microstructure and R-ratio on fatigue crack curves of Ti-6Al-4V alloy in laboratory air at 20 Hz [25].

6 Estimation of the Fatigue Curve under Closure-Free conditions in Air

It is worth noting that Liaw *et al.* [26] reviewed threshold data in air under closure-free conditions ($\Delta K_{th,eff}$) for six alloy systems including iron, aluminum, copper, magnesium, nickel, and titanium. They found $\Delta K_{th,eff}$ to be directly proportional to E regardless of its metallurgical state:

$$\Delta K_{th,eff} = 1.6 \times 10^{-5} E \tag{6}$$

where $\Delta K_{th,eff}$ is in MPa√m and E in MPa. Note Eq. (6) shown as point A in Figs. 4 to 7.

Thus, the dependence of FCGR under closure-free conditions on E is applicable for the threshold region (Stage I) as well. Recognizing that stage I rises very steeply from the threshold value, the stage I-II transition is anticipated to be near and slightly above $\Delta K_{th,eff}$. Therefore, we can construct approximately the whole fatigue curve in air (Stages I and II) for any metal under closure-free conditions as, can be seen Fig. 8. Note either Eq. (2) or Eq. (5) can be used to model stage II since the difference between the two is not that significant. It is reasonable to approximate stage I behavior by drawing a vertical straight line through point A on the conventional *log-log* plot of da/dN *vs.* ΔK. Note $da/dN = 5.43\times10^{-7}$ mm/cycle at stage I-II transition is the same for all the alloys, which can be obtained by substituting Eq. (6) in Eq. (2).

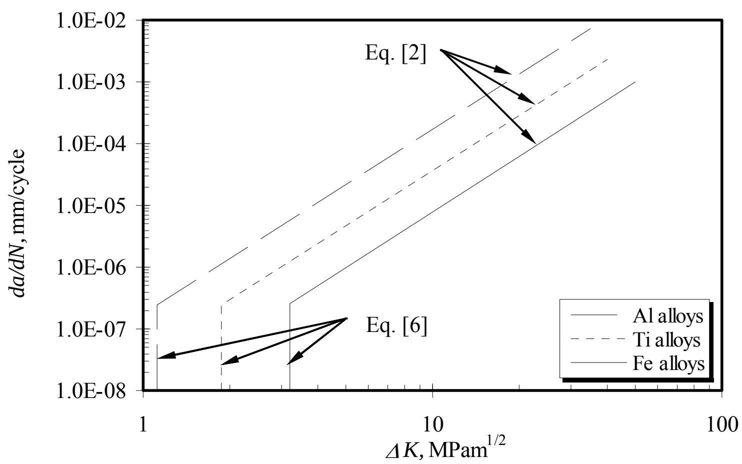

Fig. 8: Simplified fatigue curves under closure-free conditions for steel, titanium and aluminum alloys in air.

7 Implication on the Industry

Fatigue loading is a serious concern for dynamic risers and free spanning subsea pipeline used for oil and gas recovery from deep seawater. An Engineering Critical Assessment (ECA) is a procedure normally used to define tolerable flaw size in critical welded joints for risers and subsea pipelines. A number of codes provides guidance for carrying out an ECA including, BS 7910 [27] and API-RP-579 [28]. These codes utilize both fracture mechanics and fatigue crack growth analyses to determine maximum tolerable weld flaw size. A similar equation to Hertzberg's equation has been adopted for steel in BS7910. However, for non-ferrous metals, BS7910 specifies an equation that is un-necessarily expressed as a function ($E_{\mathrm{steel}}/E_{metal}$) which may be confusing when in reality the form of Hertzberg's equation should be sufficient. This is also the case for the threshold values ($\Delta K_{th,eff}$) where the equation by Liaw *et al.*, Eq. (6), should be adopted. These two points are important in view of the findings of the current work which has improved the confidence in both equations.

8 Conclusions

The fatigue literature has revealed a correlation between FCGR and the ratio $\Delta K/E$ for different metals tested under a wide range of conditions. This correlation was observed by many to be relevant to fatigue under closure-free behavior, striations and between the Paris parameters *m* and *C*. A link was made between the three correlations in this study. The results highlight and give credence to the following conclusions:

1. The notion that modifications in the alloy's composition, microstructure or mechanical properties affect the fatigue behavior, by contributing to different closure processes at low *R*-ratios and only at the threshold and near-threshold regions.
2. Considerable amount of experimental data for a wide range of metals have shown that FCGR in air under closure-free conditions can be reasonably estimated based on Young's modulus. A simplified fatigue curve under closure-free conditions is considered an upper bound for FGCR and it can be useful in design of engineering components to establish a safe life.

References

1. Paris, P. and Erdogan, F., A Critical Analysis of Crack Propagation Laws, Journal of Basic Engineering, Transactions of ASME, Dec. 1963, pp.528-534.
2. Pearson, S., Fatigue Crack Propagation in Metals, Nature, Vol. 211, no. 5053, pp. 1077-1078, Sept. 1966.
3. Lal, D. N., On the Combined Influences of Young's Modulus and Stress Ratio on the LEFM Fatigue Crack Growth Process: a New Mechanistic Approach, Eng Frac Mech, Vol. 54, no. 6, pp. 761-790. Aug. 1996 .
4. Newman, J. C., The Merging of Fatigue and Fracture Mechanics Concepts: A Historical Perspective, Conference Fatigue and Fracture Mechanics. 28th Volume; Saratoga Springs, New York; USA; 25-27 June 1996, pp. 3-51.
5. Hertzberg, R. W., On the Calculation of Closure-Free Fatigue Crack Propagation Data in Monolithic Metal Alloys, Mat Sci Eng A190, 1995, pp. 25-32.
6. Tanaka, T., Masuda, C., and Nishijima, S., The Generalized Relationship Between the Parameters *C* and *m* of Paris' Law for Fatigue Crack Growth, Scripta Metallurgica, Vol. 15, 1981, pp. 259-264.
7. Hickerson, J.P., and Hertzberg, R.W., The Role of Mechanical Properties in Low Stress Fatigue Crack Propagation, Metall. Trans. 3, 1972, pp.179-189.
8. Cavallini, M., and Iacoviello, A Statistical Analysis of Fatigue Crack Growth in a 2091 Al-Cu-Li Alloy, Int J of Fatigue, Vol. 17, No. 2, pp. 135-139, 1995.
9. Cortie, M.B., and Garrett, G.G., On the Correlation Between the *C* and *m* in the Paris Equation for Fatigue Crack Propagation, Eng Frac Mech, Vol. 30, No. 1, 1988, pp. 49-58.
10. McCartney, L.N., and Irving, P.E., Comments on "A Correlation for Fatigue Crack Growth Rate", Scripta Metallurgica, Vol. 11, 1977, pp. 181-183.
11. Iost, A., and Lesage, J., On the Existence of a Pivot Point for Stage II Fatigue Crack Growth, Eng Frac Mech, Vol. 36, No. 4, 1990, pp. 585-596.

12. Bergner, F., and Zouhar, G., A New Approach to the Correlation Between the Coefficient and the Exponent in the Power Law Equation of Fatigue Crack Growth, Int J of Fatigue, Vol. 22, 2000, pp. 229-239.
13. Sriharsha, H.K., Pandey, R.K., and Chatterjee, S., Towards Standardizing a Sub-size Specimen for Fatigue Crack Propagation Behavior of a Nuclear Pressure Vessel Steel, Eng Frac Mech, Vol. 64, No. 5, 1999, pp. 607-624.
14. Niccolls, E.H., A Correlation for Fatigue Crack Growth Rate, Scripta Metallurgica Vol. 10, 1976, pp. 295-298.
15. Baflon, J.P., and Masounave, J., On the Relationship Between the Parameters of Paris' Law for Fatigue Crack Growth in Alumimuim Alloys, Scripta Metallurgica Vol. 11, 1977, pp. 1101-1106.
16. Suresh, S., Fatigue of Materials, 2nd Ed., Cambridge University Press, 1998.
17. Suresh, S., and Ritchie, R.O., Near-Threshold Fatigue Crack Propagation: A Perspective on the Role of Crack Closure, Conference on Fatigue Crack Growth Threshold Concepts, Philadelphia, U.S.A., 3-5 Oct. 1983, The Metallurgical Society/AIME, pp. 227-261, 1984.
18. Bates, R.C., and Clark, W.G., Fractography and Fracture Mechanics, Transactions of ASM, Vol. 62, 2, 1969, pp. 380-389.
19. Data Book on Fatigue Crack Growth Rates of Metallic Materials, The Society of Materials Science, Japan, Vol. 1 and 2, 1983.
20. Handbook of Fatigue Crack Propagation in Metallic Structures, Edited by Andrea Carpinteri, Elsevier, Amsterdam, The Netherlands, vol. 1 and 2, 1994.
21. Vasudevan, A.K., and Suresh, S., Influence of Corrosion Deposits on Near-Threshold Fatigue crack Growth Behavior in 2XXX and 7XXX Series Aluminum alloys, Met. Trans A, Vol. 13A, 1982, pp.2271-2280.
22. Suresh, S., Zamiski, G.f., and Ritchie, R.O., Oxide-Induced Crack Closure: An Explanation for Near-Threshold Corrosion Fatigue Crack Growth Behavior, Met. Trans A, Vol. 12A, 1981, pp.14351443.
23. Suresh, S., Toplosky, J., and Ritchie, R.O., Environmentally Affected Near-Threshold Fatigue Crack Growth in Steels, Fracture Mechanics: 14th Symposium volume I: Theory and Analysis, ASTM STP 79, J.C. Lewis and G. Sines, American Society for Testing and Materials, 1983, pp. I-329-I-347.
24. Bucci, R.J., Development of a Proposed ASTM Standard Test Method for Near-Threshold Fatigue Crack Growth Rate Measurements, A symposium on Fracture Testing, ASTM STP 738, 1979, Hudak, S., and Bucci, R.J., pp. 5-28.
25. Chesnutt, J.C., and Wert, J.A., Effect of Microstructure and Load Ratio on ΔK_{th} in Titanium Alloys, Proceedings of the International Symposium on Fatigue Crack Growth Threshold concepts, the Metallurgical Society of AIME, Eds. D.L. Davidson and S. Suresh, Pennsylvania, 1983, pp. 83-98.
26. Liaw, P., Leax, T., and Logsdon, W., Near-Threshold Fatigue Crack Growth Behavior in Metals, Acta. Metall. Vol. 31, No. 10, pp. 1581-1587, 1983.
27. British Standard 7910: "Guide on Methods for Assessing the Acceptability of Flaws in Fusion Welded Structures.", 2005.
28. API-RP-579 - "Recommended Practice for Fitness for Service.' First Edition, 1st January 2007.